Heritage Science

RESEARCH

Open Access

Precise in-situ detection of inorganic pigments in ancient architectural color paintings by HH-XRF

Long Zhang[1], Ziyan Song[2], Shengda Zuo[2], Feng Hou[3*] and Shuaiqing Chen[4]

Abstract

The handheld X-ray fluorescence spectrometer (HH-XRF) is commonly used to detect the inorganic elemental composition of pigments on-site. However, the accuracy of in-situ detection results can be affected by the characteristics of the painted surface contaminants and the layered structure of pigments in ancient architectural color paintings. To mitigate this error, a method was proposed that combined the XRF spectra of inorganic pigments with the elemental concentration values obtained through principal component analysis (PCA). Additionally, this study discussed the typical surface contaminants and pigment layering found in color paintings separately. Firstly, experiments were conducted on dust accumulation layers of varying thicknesses. The results indicated that the condition of color paintings after pretreatment of dust accumulation tended to resemble the situation with thin dust accumulation during in-situ testing. A fitting formula was derived to establish a relationship between field testing and laboratory testing results. Secondly, experiments were conducted using various combinations of pigment layers. Based on the findings, it was hypothesized that there was a connection between XRF detection results and the maximum concentration value of a single element (as determined by XRF, in an unmixed or unlayered pigment sample without dust or smoke accumulation). The test results were fitted using a Polynomial formula, providing evidence for the existence of a nonlinear functional relationship between these two variables. Finally, an empirical formula for predicting the concentration values of the top color layer with different base colors was proposed. This study offered a precise method for accurately assessing pigments of ancient architectural color paintings through in-situ testing.

Keywords Ancient architectural color painting, Inorganic pigment, HH-XRF, In-situ testing

Introduction

Chinese ancient architectural color paintings serve both as decorative elements for ancient buildings and as protective coatings for wooden structures, guarding against dampness, rot, and woodworm. These paintings represent the aesthetic orientation, ideological values, and cultural characteristics of ancient Chinese architecture in different eras. Consequently, the examination of painting materials has garnered significant attention from heritage conservation, restoration projects, and academia.

Over time, color paintings have required repairs due to various ailments such as dust accumulation, chalking, cracking, scaling, and other forms of damage. However, in the practical restoration process, it is difficult to identify the specific pigments used in the color paintings, especially for the complex situation of layering, which causes great difficulties in the restoration of color paintings. Therefore, experimental instruments are frequently

*Correspondence:
Feng Hou
houf@tju.edu.cn
[1] School of Architecture, Tianjin University, Tianjin 300072, China
[2] School of International Engineering Institute, Tianjin University, Tianjin 300072, China
[3] School of Materials Science and Engineering, Tianjin University, Tianjin 300072, China
[4] Lowa State University, Lowa State 50011, USA

employed to assist in the identification of pigments within color paintings.

Presently, the most commonly used instruments worldwide for this purpose encompass lossy detection experiments employing techniques such as polarized light microscopy, X-ray fluorescence spectroscopy (XRF), X-ray diffraction analysis (XRD), scanning electron microscope with energy-dispersive X-ray spectroscopy (SEM–EDX), Fourier-transform infrared spectroscopy(FTIR), Raman spectroscopy, and other similar devices [1–5]. Barone et al. [1] used XRD and micro-Raman spectroscopy to test micro-samples from painted architectural slabs. Koochakzaei et al. [2] identified blue pigments used in mural paintings of Ali Qapu palace with five collected samples by polarized light microscopy(PLM), FTIR, Raman spectroscopy, and energy-dispersive X-ray spectroscopy(EDS). Zhaojun Liu et al. [3] studied 60 samples were collected on a mural painting tomb, whose pigments were analyzed by micro-Raman, FT-IR, XRD and SEM–EDX. Marrocchino et al. [4] carried out micro-samplings from the decorations of the cloister, and the samples were subjected to four different laboratory analyses: stereomicroscope and SEM–EDS observations, XRF and micro-Raman spectroscopy. Wiggins et al. [5] analyzed paint samples and cross sections from the painted ceiling decoration of Lin'xi Pavilion in the Forbidden City with SEM–EDX, time of flight-secondary ion mass spectrometry(ToF–SIMS), XRD, FTIR, and Raman spectroscopies.

Nonetheless, these paintings are delicate immovable cultural artifacts, making it impossible to remove and transport them to a laboratory for testing. Additionally, the employment of destructive or minimally destructive laboratory testing methods poses challenges for widespread implementation as they result in irreversible damage to the color paintings, failing to provide adequate protection. Furthermore, many of these laboratory instruments have high testing costs, require expensive equipment, and exhibit low testing efficiency.

On the other hand, portable X-ray fluorescence (pXRF), specifically the handheld XRF (HH-XRF), has become widely available and is extensively used for the analysis of pigments in various applications such as frescoes [6], pottery [7], plasters [8], and oil paintings [9]. The combination of pXRF with other instruments has proven effective for pigment analysis in frescoes, oil paintings, and other colored paintings [10–16]. However, there is a significant lack of research on the application of pXRF for pigment detection in ancient architectural color paintings. Therefore, a thorough investigation into the scientific methodology of HH-XRF detection for such paintings is greatly needed.

During in-situ testing of color paintings using HH-XRF, impurity signals often appear in the test results, making it difficult to determine the exact source of the elements and, consequently, accurately identify the pigments used. Several factors contribute to this issue. Firstly, the pigments themselves are not sufficiently pure and contain mineral impurities. Secondly, on-site color paintings often exhibit various surface contaminants [17], which obscure the data sources of detection and generate impurity signals. Lastly, the color paintings are layered [18, 19], with multiple layers of pigments superimposed, resulting in elemental signals from different mineral pigments.

This study aims to address the aforementioned challenges. Experimental simulations were conducted using mock-up samples of color painting boards from the Qing dynasty, incorporating surface contaminants and pigment layering. Firstly, the color-revealing elements of each pigment were determined by analyzing the XRF spectra of inorganic pigments and performing PCA on the concentration values of each element across different pigments. This information was used to identify the specific inorganic pigments. Secondly, by analyzing the concentration values of the detected elements, a formula was developed to infer the exact pigments used in cases of dust accumulation contaminants and pigment layering. This approach aims to enhance the accuracy, applicability, and scientific rigor of in-situ testing results for inorganic pigments in color paintings using HH-XRF.

The rest of this paper is organized as follows. We start with the introduction of the experimental procedures and test methods of mock-up samples of color painting boards in Sect. "Method". We then describe the results of multiple experiments and propose an accurate testing method based on a single instrument in Sect. "Results". The advantages and limitations of our method are described in Sect. "Discussion", and Sect. "Conclusion" concludes the paper.

Method

Mock-up samples of color painting board

The experimental painting board used in this study was a Korean pine block measuring 20 cm × 20 cm × 1 cm. The surface of the wood block was coated with a single layer of plaster, adhered with traditional bone glue. The bone glue is boiled with animal bones, which are nitrogenous organic substances, belonging to the protein group and cannot be detected by an XRF analyzer. The pigment samples were provided by Beijing Yuquan Ancient Building Painting and Decoration Co., a construction unit specializing in the restoration of ancient buildings for the Summer Palace Administration.

The main colors chosen for the experiments were derived from inorganic pigments of seven colors: red, yellow, blue,

green, white, black, and gold. These pigments included cinnabar (HgS, the natural mineral), vermilion(HgS, synthetic material), minium (Pb_3O_4), hematite (Fe_2O_3), realgar (As_4S_4), chrome yellow ($PbCrO_4$), earth yellow (α-FeOOH), azurite ($2CuCO_3{\cdot}Cu(OH)_2$), ultramarine ($(Na, Ca)_8(AlSiO_4)_6(SO4, OH, S, Cl)_2$) [20], malachite ($CuCO_3{\cdot}Cu(OH)_2$), Paris green ($[Cu(CH_3COO)_2{\cdot}3Cu(AsO_2)_2]$), lead white ($mPbCO_3{\cdot}nPb(OH)_2$), titanium white ($TiO_2$), carbon black ($C_5$), red gold (Au, 74% gold content), and ku gold (Au, 98% gold content). In total, there were 13 pigments and 2 types of gold paste. Small colors [18, 19] were used for smaller volume parts and demitint colors [[18, 19] were produced by mixing the aforementioned pigments. The demitint colors included er green (malachite and lead white), san green (Paris green and lead white), er cyan (azurite and lead white), san cyan (azurite and lead white), pink (realgar and lead white), and greenish yellow.

In general, 14 boards were created. 7 in the first row were layered designs, classified into overlaying of different pigments and overlaying of the same pigment, and 7 in the second row were 6 painting boards of single layer and 1 board of ground layer.

In Experiment 1, a total of 11 boards were prepared for dust collection, each representing a specific pigment: 5 from row one of overlaying of the same pigment–malachite, azurite, ultramarine, hematite and minium, 6 from row two–lead white, titanium white, realgar, chrome yellow, earth yellow and the ground layer. Then the dust on the board was cleared out, and a total of 10 boards were used to perform the incense experiment, each representing a specific pigment: malachite, azurite, ultramarine, hematite, minium, lead white, titanium white, realgar, chrome yellow and earth yellow.

In Experiment 2, base colors of green, blue, and red were chosen, and additional pigments were applied to them according to the principles of color painting. The color painting board was layered with pigments of the same thickness. 7 color boards were created (in row one), including two green color boards (malachite and Paris green), two blue color boards (azurite and ultramarine blue), and three red color boards (minium, hematite and cinnabar). The 7 boards in row two were also tested in Experiment 2. The mock-up samples of the color painting board are depicted in Fig. 1.

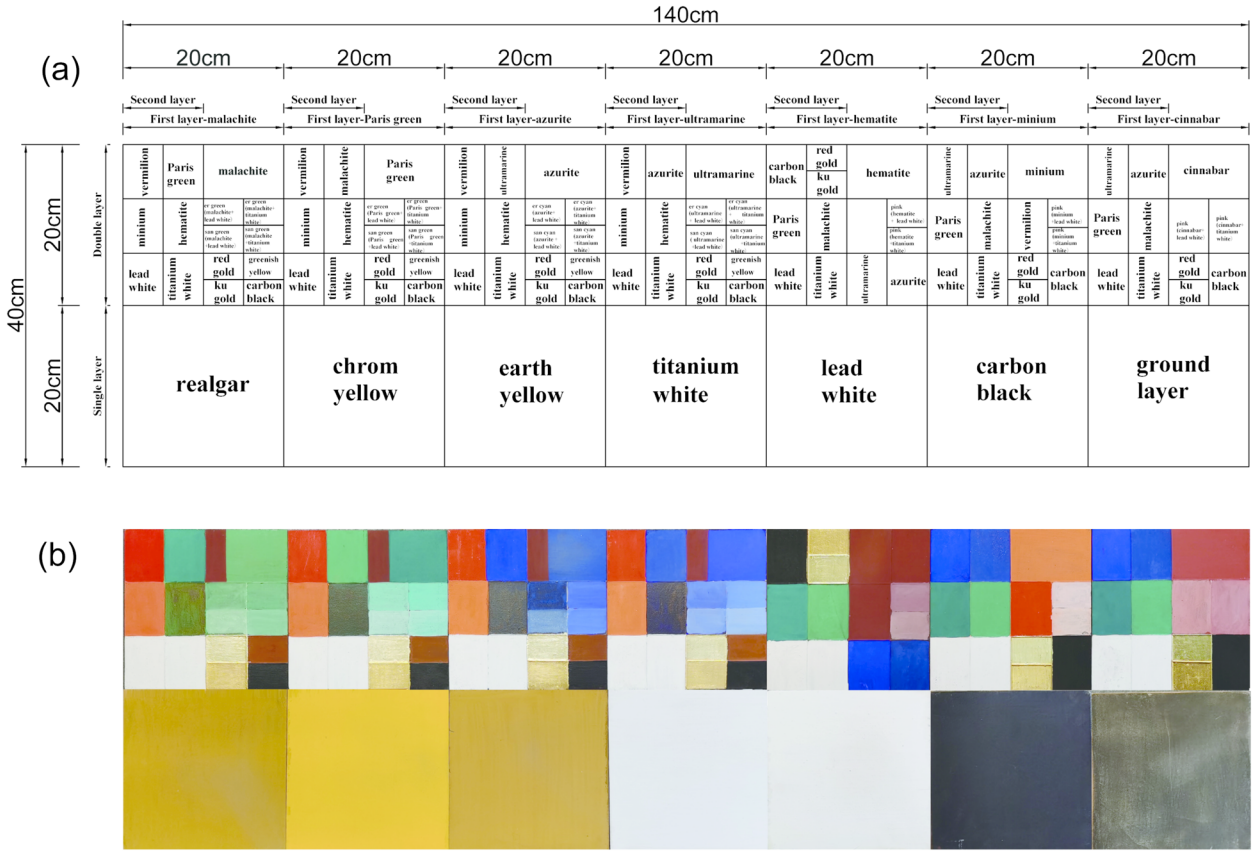

Fig. 1 Mock-up samples of color painting board. **a** Location of specific pigments. **b** Photo of color painting boards

Experiment

The error of the color painting test can be categorized into two types. The first one is that the color paintings are exposed to the outdoor environment over a long time and thus the surface contaminant is produced. In particular, the accumulation of dust due to atmospheric precipitation and smoke due to the use of architectural scenes such as places of worship, both of which greatly affect the accuracy of XRF in-situ tests. In the other type, it is common for colored paintings to have multiple layers of pigments superimposed due to the method of painting in layers, however, the overlay causes a huge dilemma in XRF testing, and the test results often differ greatly from the standard pigments. Therefore, this study replicates both of these possible error-causing situations under laboratory conditions, and the specific details of the experiment are as follows:

Experiment 1: detection of the effect of typical surface contaminants on elemental concentrations

(a) Dust accumulation experiment

The dry dust [21, 22] utilized in this experiment primarily consisted of natural dust collected using the dry dust collection method.

To minimize the impact of airborne dust, the 11 color painting boards were positioned adjacent to each other at a height of 0.8 m from the ground outside the laboratory window.

A protective fence was erected around the painted boards to prevent the collected dust on the surface of the painted boards from being dispersed by wind.

The dust accumulation on the painted boards was regularly monitored throughout the experiment. Outdoor dust collection commenced in March and concluded in June, encompassing two different conditions: thin dust accumulation (after 2 months of collection) where the pigment layer was still visible to the naked eye, and thick dust accumulation (after 4 months of collection) where the pigment layer was completely obscured and no longer discernible. Three test points were selected evenly from the smooth surface on the centerline of the 11 boards. Each point underwent three separate detections, with each detection lasting 60 s. The final results were obtained by averaging the readings.

(b) Incense experiment

In the incense experiment, five incense pillars will be lit on the ground, with a 30 cm high tin enclosure around it to become an enclosed space and leave the top as a ventilation hole. Painted board covered with an iron fence, about 30 cm away from the incense pillars. Five incense pillars were placed at a time, which were replaced promptly after burning out, and the incense smoke was observed every hour. Test points were selected from the smooth surface of the 5 boards, which were selected evenly from the smooth surface on the centerline of each board. Three separate detections were carried out on each point, with each detection lasting 60 s. The final results were obtained by averaging the readings.

Experiment 2: detection of the effect of pigment layered on element concentration

The testing process involved conducting separate tests on five boards, following a specific detection order: the base color was detected first, followed by the other pigments layered on top. For each board, three test points were chosen evenly on the centerline of the board. Each point on the complete smooth surface was tested three times, with a detection time of 60 s per test. The final results were obtained by averaging the readings from the three tests conducted on each point.

The experimental conditions of the above three experiments and the color painting drying process were all strictly protected from light, and the degradations of pigments caused by air pollution and light were negligible.

Handheld X-ray fluorescence analysis

X-ray fluorescence analyses were conducted on specific points of the color painting boards using a Niton XL2–960 GOLDD XRF spectrometer (Thermo Fisher Scientific, Niton, America). This instrument is equipped with an Ag-anode tube, capable of reaching a maximum voltage of 45 kV and a maximum current of 100 μA, using beam filters called collimators, but without using a vacuum pump and helium atmosphere.

Under these working conditions, the radiation intensity of X-rays is very weak, so the X-ray does not cause damage to the paintings. The penetration depth of an X-ray can reach a centimeter level, and the thickness of the pigment layer is much lower than the penetration depth of an X-ray, thus HH-XRF is applicable to this experiment. There are two instrumental modes (Soils, Mining: Cu/Zn, Mining: Ta/Hf) for particular analytes. In the Soil mode, there is only a main filter and the following elements could be detected: Ba, Sb, Sn, Cd, Ag, Pd, Zr, Sr, Rb, Pb, Au, Se, As, Hg, Zn, W, Cu, Ni, Co, Fe, Mn, Cr and Ti. In the Mining mode, the filters for each irradiation session include the main range and light range. The filters are set to include the following elements: Main: Ba, Sb, Sn, Cd, Pd, Ag, Sb, Sn, Cd, Pd, Ag, Mo, Nb, Zr, Sr, Rb, Bi, As, Se, Pb, W, Zn, Cu, Re, Ta, Hf, Ni, Co, Fe, Mn, Cr, V, Ti. Light: Ca, K. Al, P, Si, Cl, S, and Mg. It also features a geometrically optimized large-area drift detector (GOLDD). During the analysis,

the HH-XRF method was employed, whereby the front end of the spectrometer was gently placed in direct contact with the painted surfaces.

The Soils mode is used to measure the elements lower than 0.5%, while the Mining mode is more suitable to the elemental content greater than 0.5%. In the present analysis, the contents of the main elements were higher than 1%, and there was no Ta/Hf in the pigments. Therefore, Mining: Cu/Zn was selected as the mode. The instrument software provided element quantifications based on a built-in algorithm (combining fundamental parameters and empirical coefficients) with the measurement units set to weight percent (%) for the Mining mode. Each measurement had an acquisition time of 60 s (30 s for each of the main and light filters). The X-ray spot diameter on the sample was 8 mm, and precise positioning on the targeted analysis point was achieved using an integrated camera. The term "color-revealing elements" is used to describe elements in XRF spectra that align with the characteristic elements of pigments.

Results

Elements analysis of each inorganic pigment

Color-revealing elements

The color-revealing elements of each pigment are identified by analyzing the characteristic XRF spectra, considering the characteristic elements in the chemical formula and the main elemental composition determined by XRF measurements.

The XRF spectra analysis results for each pigment in the mock-up samples of the color painting board are presented in Fig. 2. In Fig. 2a, Cu is the color-revealing element in malachite (green pigment) and azurite (blue pigment), exhibiting distinct peaks with no other impurities. Similarly, other color-revealing elements include Ti in titanium white, Pb in lead white, Pb and Cr in chrome

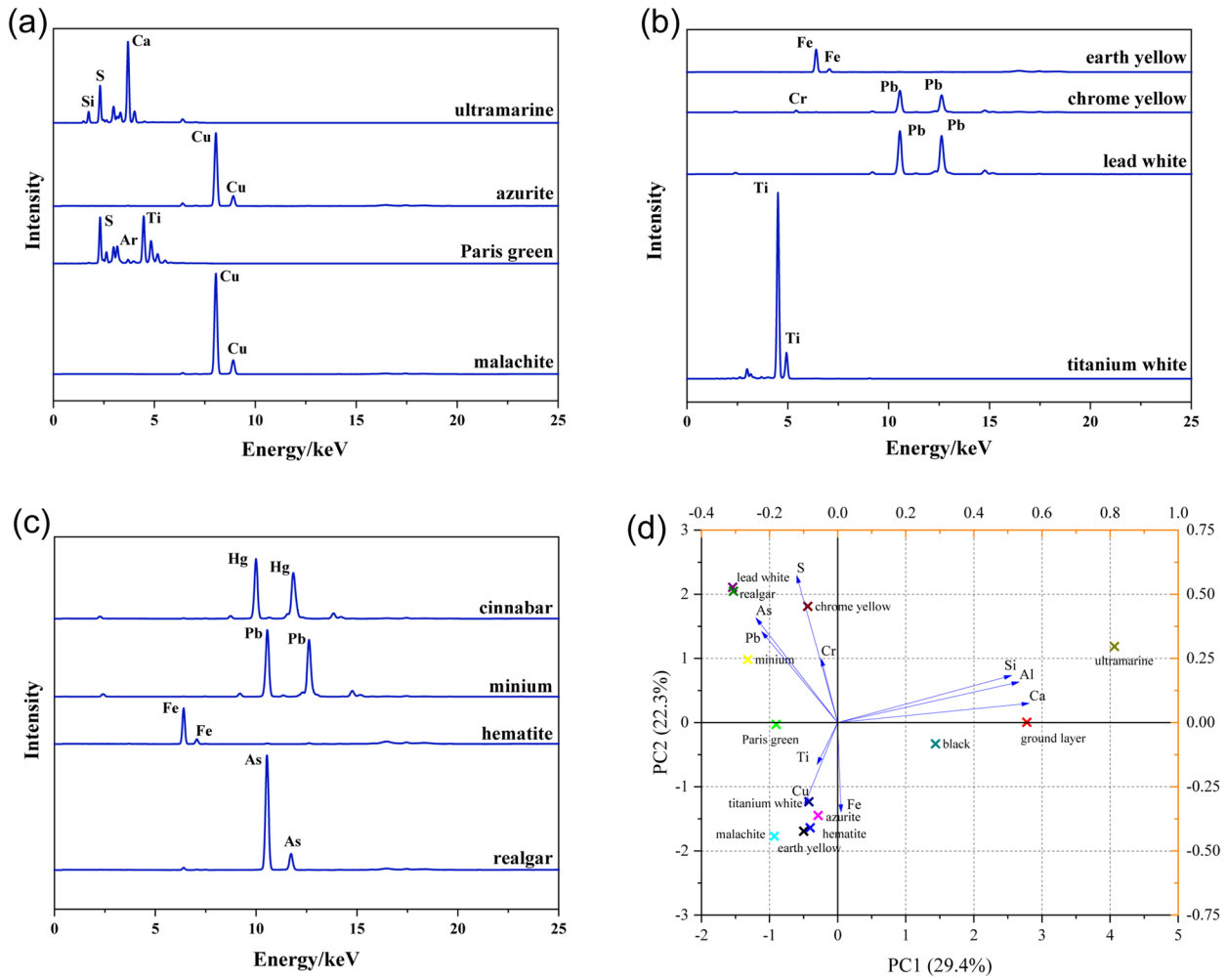

Fig. 2 Color-revealing elements analysis of each inorganic pigment. XRF spectra of (**a**) malachite, Paris green, azurite and ultramarine. **b** lead white, titanium white, chrome yellow and earth yellow. **c** realgar, hematite, minium and cinnabar. **d** Principal component analysis of elements

yellow, Fe in earth yellow, As in realgar, Fe in hematite, Pb in minium, and Hg in cinnabar. However, the characteristic XRF spectra of ultramarine ($Na_6Al_4Si_6S_4H_{20}$) are unclear, lacking clear color-revealing elements for accurate identification. Additionally, the characteristic XRF spectra of Paris green (Ti, V) do not match the expected elements of Paris green (Cu, As), indicating that the Paris green detected in this experiment does not contain Cu or As. The cinnabar and vermilion (using Soils mode of HH-XRF) were excluded due to the inability to measure mercury (Hg) using the same mode (Mining mode) of the HH-XRF analyzer as the other pigments. And HH-XRF analyzer cannot detect C, so carbon black was excluded. Moreover, there are no characteristic peaks in the results for the elements of red gold and ku gold, resulting in the exclusion of these pigments from subsequent analysis.

PCA analysis was performed on the concentration value data of each element obtained by HH-XRF. Figure 2d showed that the first two principal components (PC1, PC2) accounted for 29.4% and 22.3% of the variance, respectively. Firstly, the pigments were represented as points whose coordinates represented the score in PC1 versus PC2. Secondly, the elements were illustrated by load vectors, whose direction was positively correlated with the two principal components if it coincided with the direction of the coordinate axes of the two principal components, while the distance could be considered as the degree of correlation. Therefore, the main elemental composition of each pigment can be determined based on the distance between the pigment point and the load vectors. The inorganic pigments are divided into four groups based on their different principal components. For instance, the main components of the group comprising lead white, realgar, minium, and chrome yellow are influenced by As, Pb, Cr, and S. Taking chrome yellow as an example, it falls on the loading vector of S and Cr, indicating that the main components of chrome yellow are S and Cr, with As and Pb as secondary main elements.

It should be noted that although the main components determined by PCA may be the same for different pigments, they can still be distinguished by the concentration values of the main elemental components, as they differ. Considering that PCA may have errors when dealing with limited data, it is necessary to consider both its results and the analysis of XRF spectra to accurately determine the color-revealing elements of each pigment. Therefore, the color-revealing elements of each pigment can be obtained as shown in Table 1.

Table 1 Color-revealing elements of each inorganic pigment

Color	Inorganic pigment	Color-revealing elements
Green	Malachite	Cu
	Paris green	Cu, As
Blue	Azurite	Cu
	Ultramarine	Ca, Si
Red	Minium	Pb
	Hematite	Fe
Yellow	Realgar	As
	Chrome yellow	Pb, Cr
	Earth yellow	Fe
White	Lead white	Pb
	Titanium white	Ti
Ground layer	Ca, Si, Al, Fe, Ti	

Correlation analysis of elements in pigments

Figure 3 depicts the elemental correlations among inorganic pigments using a heatmap. Considering the nonlinear and complex relationship between pigment element concentrations, the study employed the Spearman correlation analysis [23–24]. The results indicate that As exhibits a strong positive correlation with S and Cr, as well as a strong negative correlation with Fe and Ti. Pb shows a strong positive correlation with Cr and a strong negative correlation with Cu, while the remaining elements' correlation results are presented in Fig. 3.

The correlation analysis results provide additional insight into the phenomenon of multiple element concentrations observed in the loadings plot of the principal component analysis. In essence, the correlation study aids in examining the impact of surface contaminants on color paintings in terms of elemental aspects. It facilitates an understanding of the surface contaminants mechanism not only through changes in element concentrations caused by the surface contaminants but also through alterations in the relationship between elements.

Experiment 1: effects of typical color painting surface contaminants on element concentration

Effect of dust accumulation on elemental concentration

To examine the impact of dust accumulation on the data results, two scenarios were considered: thin and thick dust accumulation (as explained in Sect. "Experiment 1: detection of the effect of typical surface contaminants on elemental concentrations"). A comparison was made between these cases and the data obtained from pigments without dust accumulation.

In Fig. 4, it is evident that dust accumulation primarily affects the concentrations of Fe, Ca, Al, and Si [25–26], demonstrating a clear positive correlation. This implies that as the thickness of dust increases, the concentrations of these four elements also increase. Additionally, it can be observed that dust accumulation predominantly

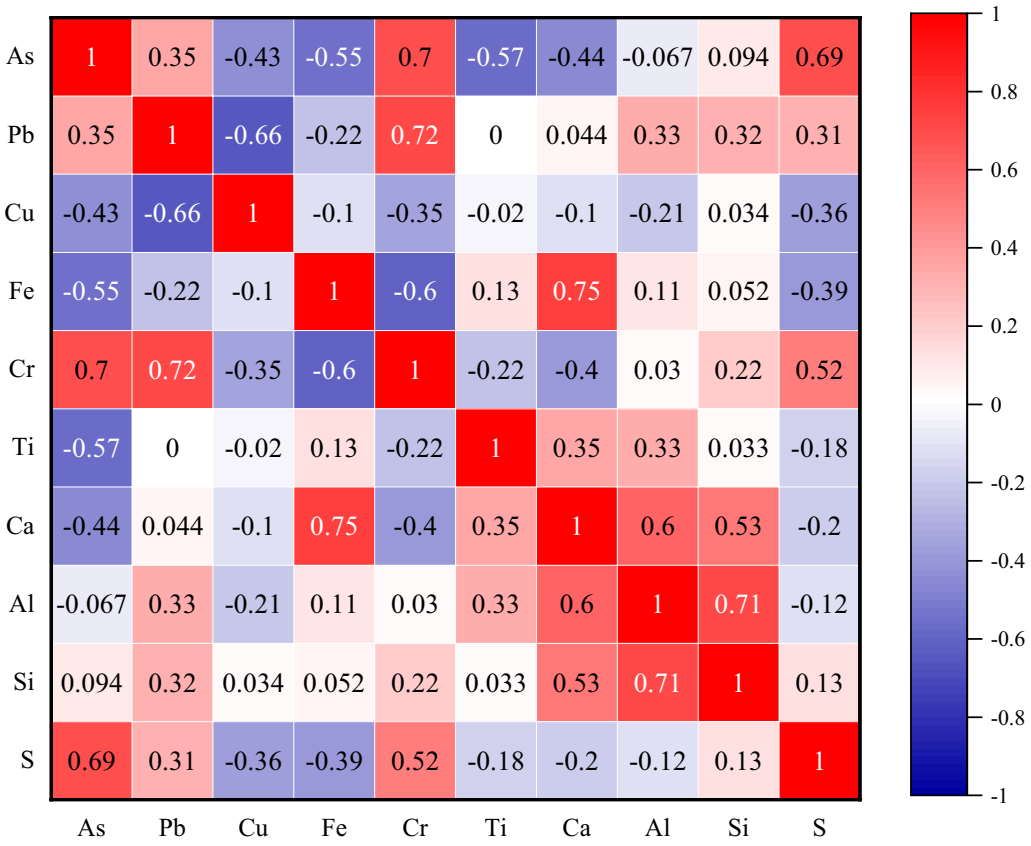

Fig. 3 The heatmap of elemental correlations in inorganic pigments

consists of Fe, Ca, Al, and Si. Furthermore, the presence of dust enhances the correlation between Ca, Al, and Si when analyzing the relationship between these elements. Interestingly, this situation does not impact the content of Fe; instead, it reduces the correlation between Fe and Ca.

Based on the test results shown in Fig. 5 for malachite and hematite, it is evident that in the presence of thick dust accumulation, the concentration of Fe, Ca, Si, and Al in the pigment tends to resemble the test results obtained for these elements in the dust itself. Similar patterns can be observed for other pigments as well. Although Ca, Si, and Al are not considered color-revealing elements for pigment identification, the presence of accumulated dust can significantly impact the analysis of hematite and earth yellow, where Fe serves as the color-revealing element. Hence, when conducting on-site testing of color paintings, pretreatment should involve the removal of surface dust from the tested points using air blowing.

Nevertheless, despite pretreating the color painting to minimize dust accumulation, it is difficult to completely eliminate dust. It is observed that, after the pretreatment, the majority of the test results tend to align with the outcomes of cases with thin dust accumulation. The fitted curve illustrating this trend is presented in Fig. 6.

Effect of incense on elemental concentration

It can be seen in Fig. 7 that the amount of incense does not have an impact on elemental concentrations. There is a weak correlation between the incense amount and the other elements, indicating that an increase in the incense amount does not result in a significant change in the concentration of the other elements. However, when comparing Fig. 3 with Fig. 7, it can be observed that the presence of impurities[27–28], particularly in the elements Ca, Si, and S, still alters the relationship between elemental concentrations after smoking. Since the smoke does not affect the elemental concentrations of the color pigments, there was no fitting performed for elemental concentrations.

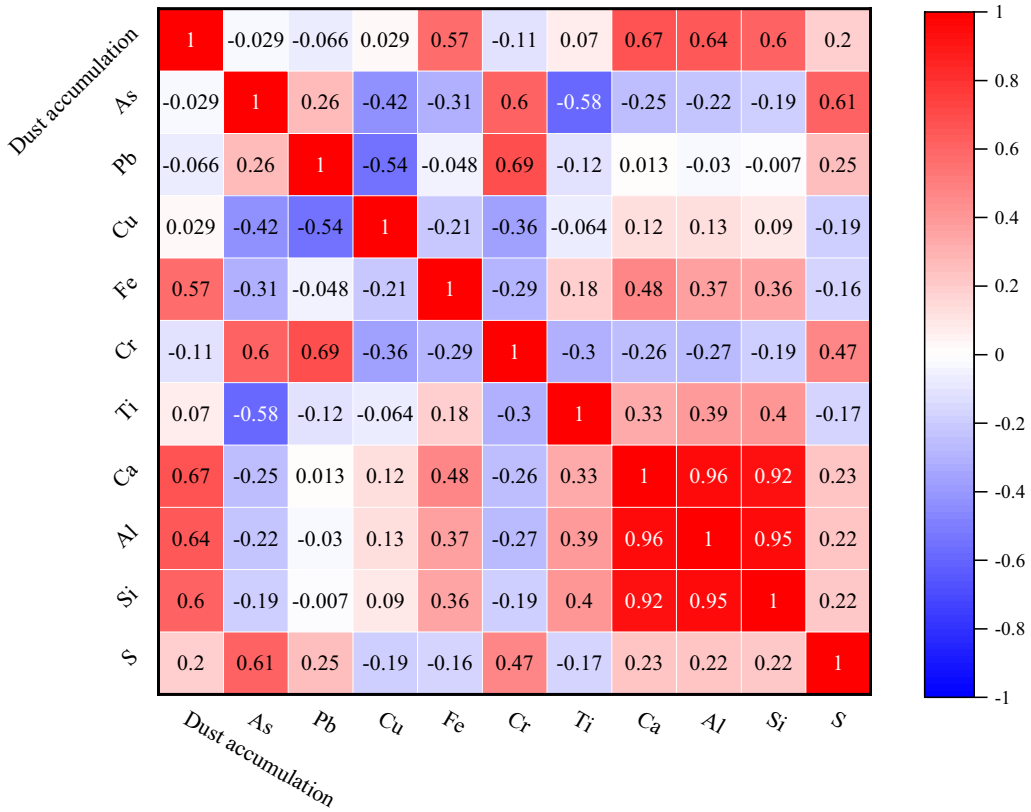

Fig. 4 The heatmap of elemental correlations in inorganic pigments under the influence of dust accumulation

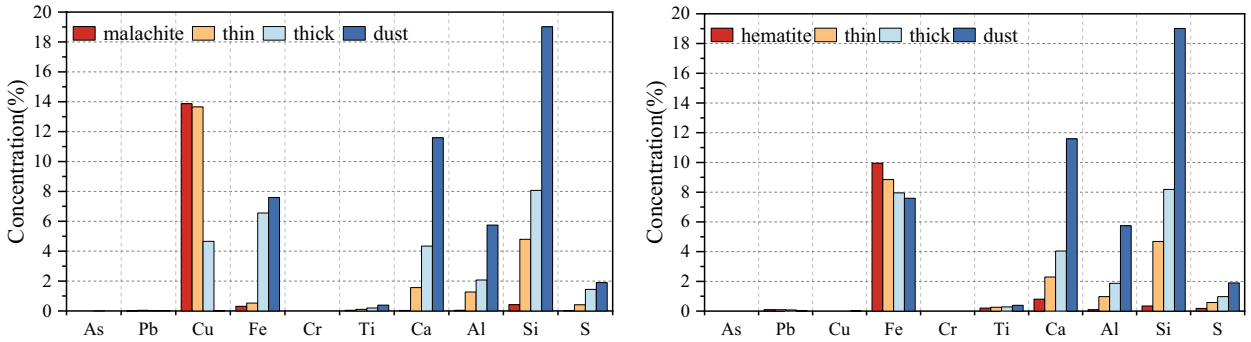

Fig. 5 Elements concentration of pure pigment, thin dust accumulation, thick dust accumulation and dust

Experiment 2: effect of pigment layered on element concentration

Formulation of the basic assumption

Statistical analysis was conducted using the data obtained from crossover experiments involving various commonly used pigments in color painting. Figure 8 displays the results for the layered combination with malachite as the base and hematite as the top layer. It can be observed that the concentration values of Cu and Fe of the layered combination were closer to the larger value after comparing the concentration values of Cu and Fe in the two single-layer pigments. This pattern was consistently observed in multiple experimental sets, leading to the following assumption: there exists a relationship between the XRF test results and the maximum concentration value of an individual element(as

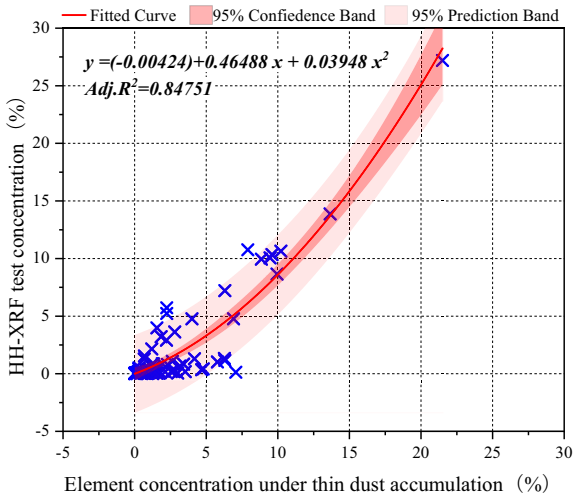

Fig. 6 Relationship between elemental concentration and XRF test results when dust accumulation is thin

determined by XRF, in an unmixed or unlayered pigment sample without dust or smoke accumulation). Consequently, this relationship is further explored in the subsequent analysis.

Study of the relationship between the max value and the XRF test results

In order to validate the assumptions proposed in subsection "Formulation of the basic assumption", all test results were subjected to fitting using the Polynomial formula. The fitting outcomes are illustrated in Fig. 9. The fit demonstrates a satisfactory R^2 value of 0.92, meeting the required criteria. This confirms the presence of a nonlinear functional relationship between the two variables and establishes a theoretical basis for the subsequent prediction and reduction of the layered form.

The prediction method and validation of pigment layered based on HH-XRF test data

The empirical formula derived in Sect. "Study of the relationship between the max value and the XRF test results" relies on prior knowledge of the pigment type before layering. The concentration of the HH-XRF test result is calculated using the maximum value of the known element concentration. While this formula demonstrates good fitting results, the practical application often requires the opposite approach. In practice, the layered results need to be determined based on the data obtained from testing. This information is crucial for assisting in the repair and conservation of color paintings.

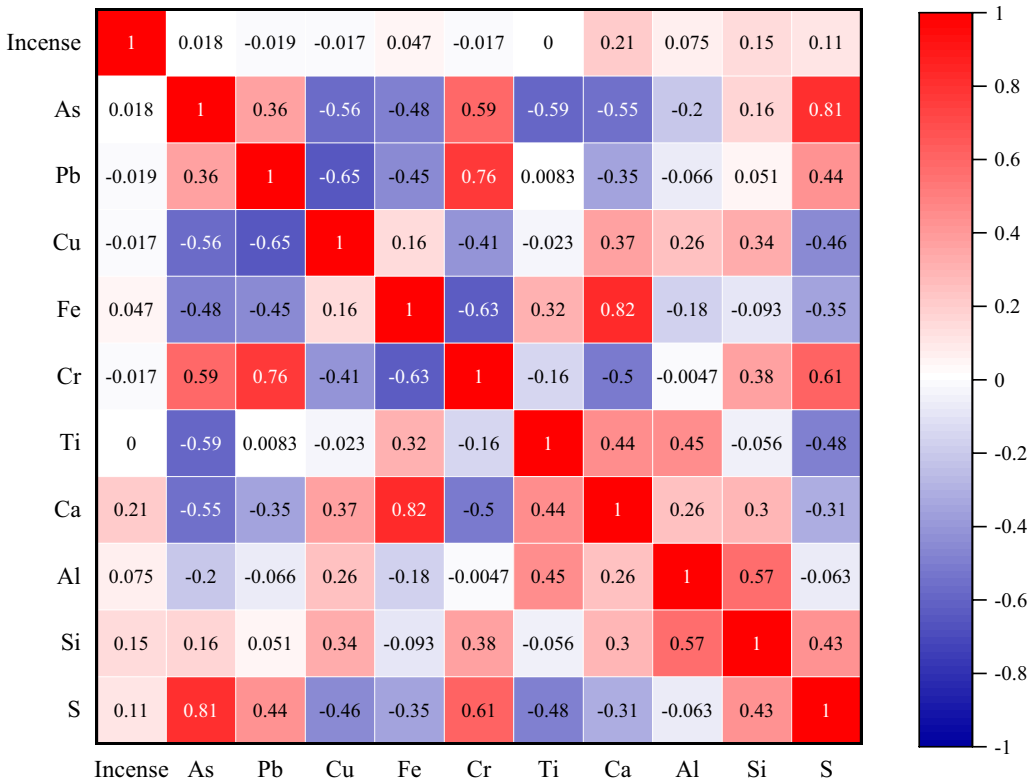

Fig. 7 The heatmap of elemental correlations in inorganic pigments under the influence of incense

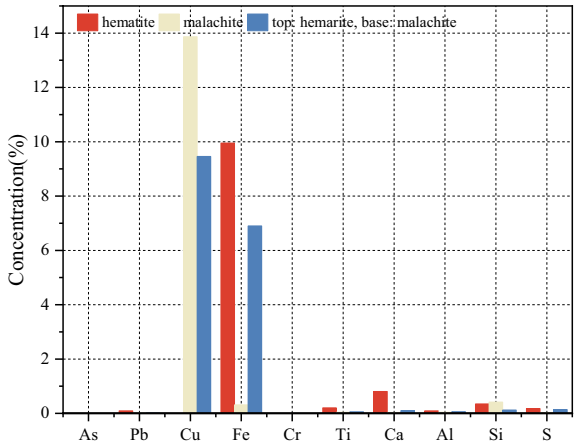

Fig. 8 Test results of pigment layered

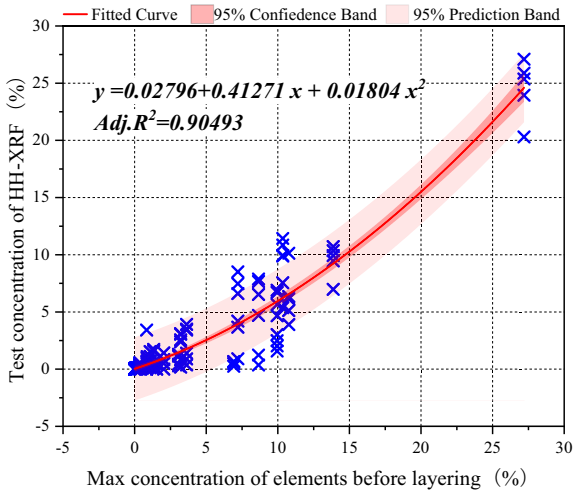

Fig. 9 The relationship between max element concentration and XRF test results

Therefore, in this section, the true value of the top color is first determined when the bottom color is known. For instance, the composition of the bottom color can be ascertained through the nearby points where damage has occurred. Based on this information, we further deduce the specific composition of both the top and bottom colors when the information regarding both colors is unknown.

Notably, in the empirical formulas depicted in Fig. 10, a significant observation is that the form of the empirical formula transitions from a nonlinear polynomial to a linear equation when ultramarine is utilized as the base color. The fitted equations mentioned above all exhibit R^2 values above 0.9, with a focus on excellent fitting results around 0.93. However, it is crucial to highlight that these accurate predictions are based on the prerequisite that the base color is known, imposing a relatively stringent requirement.

In practical applications, there is often a challenge of dealing with a "double-blind" scenario, where both the top and base colors are unknown. To address this issue, a general empirical formula is required. Figure 11 demonstrates the prediction of the maximum value of mixed pigments based on the HH-XRF test results. To ensure the accuracy of the prediction, the empirical formula was modified from the polynomial form used in the previous study to the allometric form. The fitted R^2 values met the required level of accuracy. This method relies on reducing the elemental concentration values obtained from the test to a set of maximum elemental concentration values. By comparing this set with the standard elemental concentration values for each element, the composition of the two layers of pigments can be determined, enabling the identification of the pigments in each layer.

Figure 12 displays the residual test results of the aforementioned empirical formula. The majority of residuals are concentrated around 0, indicating the accuracy and reliability of the prediction method for color painting layers.

In specific cases where the top layer consists of Pb-containing pigments like lead white and minium, the elemental information of the bottom layer is challenging to detect using HH-XRF. This is due to the strong presence of Pb, which hampers the detection, and the attenuation effect of X-rays [29]. Therefore, it becomes necessary to employ a different detection instrument in such instances.

Discussion

Painting pigments can be identified by lots of laboratory tests, whose samples are collected by scalpel [3, 4, 30] from the surface of the paintings, which can cause irreversible damage to the color paintings and cannot protect them. However, Chinese ancient architectural color paintings are fragile and immovable cultural relics, it is inappropriate to sample them and bring them to the laboratory for test. Therefore, as a portable and in-situ nondestructive testing method, our method can achieve the goal of determining the exact inorganic pigment.

In another hand, many studies [31–33] used multiple portable instrument cross-validation methods, however, which significantly increases the cost of use and more strict testing conditions. In addition, although these methods eliminate the error of the equipment, the error introduced by the test object itself still exists. Our approach considered the error characteristics and

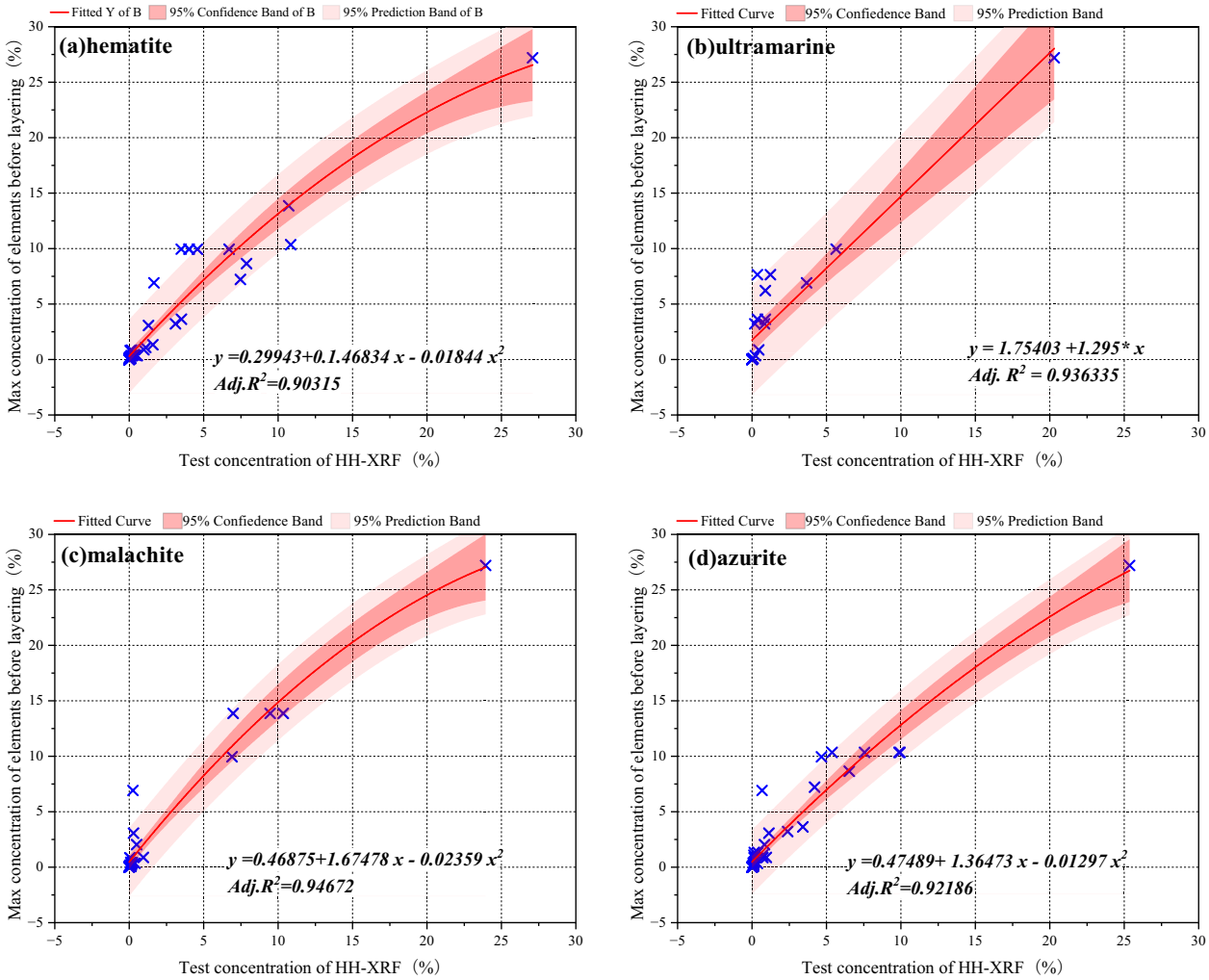

Fig. 10 Empirical formulas for predicting the concentration values of the top color with different base colors. Base colors: **a** Hemaite. **b** Ultramarine. **c** Malachite. **d** Azurite

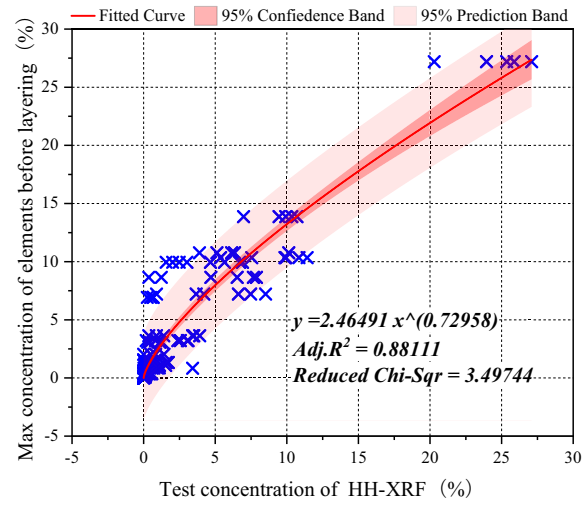

Fig. 11 Empirical formula for predicting the top color concentration values with different base colors

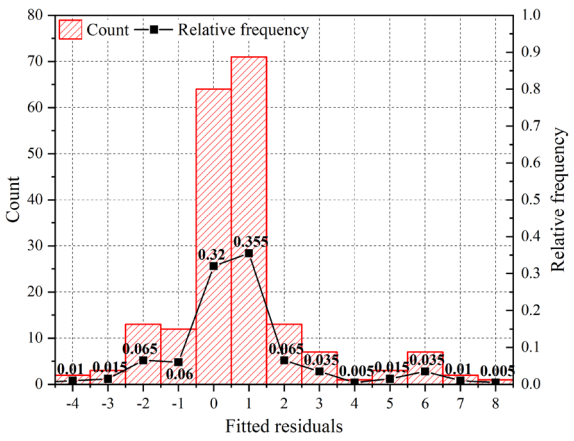

Fig. 12 Residual test of fitted curves

proposed a single-instrument in situ detection method based on HH-XRF, which effectively avoids the aforementioned unfavorable conditions. Moreover, HH-XRF has more advantages in identifying inorganic pigments in Chinese ancient architectural color paintings compared to the Raman spectrometer, which is generally considered the best way to identify inorganic pigments in paintings. Because there exists the phenomenon of pigment layering, the Raman peak spectrum presents the results of various substances superimposed on each other, which is not conducive to rapid analysis. While in the on-site test, we can judge the specific pigments according to the elemental detection results of HH-XRF.

We assume that the error is related to the thickness of the accumulated dust layer and the incense layer, but in the experiment, the thickness of them is measured by the length of time. This assumption is inadequate, and the relationship between thickness and time may be nonlinear, which is still worthy of subsequent discussion. Moreover, considering the use of pigments in color painting, some pigments have been neglected, such as red gold and ku gold, and this part of the study needs to be more in-depth.

Conclusion

HH-XRF is a portable and reliable instrument commonly used for in-situ analysis of elements in inorganic pigments in ancient architectural color paintings. However, due to the presence of surface contaminants and layered pigments in color paintings, there can be errors in the in-situ testing results. To enhance the accuracy of in-situ detection, this study utilized mock-up samples of color painting boards with Qing dynasty inorganic pigments to simulate typical color painting surface contaminants and pigment layering in the laboratory. The findings of this study can be summarized as follows:

Determination of Color-Revealing Elements: By analyzing the XRF spectra of inorganic pigments and the concentration values of each element using PCA analysis, the color-revealing elements of each pigment were identified.

In light of the conclusions, the following scientific recommendations are provided for the application of HH-XRF in in-situ measurements:

- Dust Accumulation Contaminant: In cases of thick dust accumulation, the Fe, Ca, Si, and Al elements in the detected pigments tend to exhibit similar concentrations to those found in the dust, thereby affecting pigment identification. To mitigate this error, pre-treatment involving air-blowing on the accumulated dust before in-situ testing is recommended. It is observed that the test results after this treatment tend to align with the laboratory test results for thin dust accumulation. Subsequently, specific pigments can be inferred by employing the fitting formula in Sect. "Effect of dust accumulation on elemental concentration" and considering the standard pigment concentrations.
- Incense Contaminant: The presence of impurities after incense does not alter the concentrations of pigment elements, although it affects the relationship between these concentrations. Consequently, during in-situ testing, incense can be directly detected without impacting the elemental concentrations of the pigments.
- Pigment Layering: Through the fitting of detection results using the Polynomial formula, a non-linear relationship between the XRF test results and the maximum concentration value of a single element was demonstrated. An empirical formula for predicting the elemental concentration of top layers under different base pigments was proposed. By combining the formula in Sect. "The prediction method and validation of pigment layered based on HH-XRF test data" with the standard pigment concentrations, the specific pigments used in the color painting can be inferred during in-situ testing.

Acknowledgements
Not applicable.

Author contributions
All the authors contributed to the present work. Firstly, SZ, ZS and LZ planned and conducted the experiments and collected the data. ZS and SZ performed the data analyses and wrote the article. SC assisted in experiment 1. FH supervised the entire process and provided constructive advice. All the authors read and approved the final manuscript.

Funding
This work was supported by the National 13th Five-Year Plan "Research and Demonstration of Key Technologies for Scientific Cognition and Ontological Protection of Ming and Qing Dynasty Official Building Construction Techniques" (No.2020YFC1522400).

Availability of data and materials
Data and analysis collected during the study are available from the authors upon reasonable request.

Declarations

Competing interests
The author declares that they have no competing interests.

Received: 16 July 2023 Accepted: 25 October 2023
Published online: 01 November 2023

References

1. Giorgi L, Nevin A, Nodari L, Comelli D, Alberti R, Gironda M, Mosca S, Zendri E, Piccolo M, Izzo FC. In-situ technical study of modern paintings part 1: The evolution of artistic materials and painting techniques in ten

paintings from, 1889 to 1940 by Alessandro Milesi (1856–1945). Spectrochim Acta Part A Mol Biomol Spectrosc. 2019;219:530–8.
2. Barone G, Fugazzotto M, Mazzoleni P, Raneri S, Russo A. Color and painting techniques in Etruscan architectural slabs. Dyes Pigm. 2019;171: 107766.
3. Koochakzaei A, Hamzavi Y, Mousavi MA. Characterization of the mural blue paintings in ornamental motif of Ali Qapu palace in Isfahan, Iran, using spectroscopic and microscopic methods (a case study). J Archaeol Sci Rep. 2022;45: 103632.
4. Liu Z, Yang R, Wang W, Xu W, Zhang M. Multi-analytical approach to the mural painting from an ancient tomb of Ming Dynasty in Jiyuan, China: characterization of materials and techniques. Spectrochim Acta Part A Mol Biomol Spectrosc. 2022;279: 121419.
5. Marrocchino E, Telloli C, Grazia Paletta M, Leis M. Vaccaro, the mural paintings of the cloister in the Certosa di Calci, Pisa. J Archaeol Sci Rep. 2022;43: 103461.
6. Wiggins MB, Liu M, Matsen C, Liu C, Booksh KS. Characterization of green paints in ming and qianlong dynasties' Lin'xi Pavilion by complimentary techniques. Molecules. 2021. https://doi.org/10.3390/molecules26020266.
7. Argote DL, Torres G, Hernández-Padrón G, Ortega V, López-García PA, Castaño VM. Cinnabar, hematite and gypsum presence in mural paintings in Teotihuacan Mexico. J Archaeol Sci Rep. 2020;32: 102375.
8. Izzo F, Ciotola A, Guarino V, Verde M, Bonis AD, Germinario C, Capaldi C, Morra V. Focusing on red and black engobes in Roman pottery from Cumae (southern Italy): Pompeian Red Ware and Graue Platten ceramic productions. J Archaeol Sci Rep. 2023;47: 103778.
9. Coccato A, Mazzoleni P, Spinola G, Barone G. Two centuries of painted plasters from the Lateran suburban villa (Rome): investigating supply routes and manufacturing of pigments. J Cult Herit. 2021;48:171–85.
10. Molari R, Appoloni CR. A study by portable X-ray fluorescence (pXRF) of the painting "Still Life with Vase, Plate and Flowers" (1886–1888). Appl Radiat Isot. 2023;196: 110779.
11. S.A.o.C.H.o.t.P.s.R.o. China, Diseases and legends of polychrome paintings on historic buildings, in, Cultural Relics Press, Peking, 2010.
12. Bian JY. Chinese ancient architecture color painting. Peking: China Building Materials Industry Press; 2007.
13. Schnetz K, Gambardella AA, van Elsas R, Rosier J, Steenwinkel EE, Wallert A, Iedema PD, Keune K. Evidence for the catalytic properties of ultramarine pigment. J Cult Herit. 2020;45:25–32.
14. Jiang GQ. Chinese Qing Dynasty official architecture color painting technology. Peking: China Architecture and Architecture Press; 2005.
15. Prion S, Haerling KA. Making sense of methods and measurement: spearman-rho ranked-order correlation coefficient. Clin Simul Nurs. 2014;10:535–6.
16. Akoglu H. User's guide to correlation coefficients, Turkish. J Emerg Med. 2018;18:91–3.
17. Tang Y, Han GL, Xu ZF. Mineral composition characteristic of natural atmospheric dust in Beijing and Northern areas to Beijing, Bulletin of Mineralogy. Petrol Geochem. 2011;30:150–5.
18. Guo XH, Gao RY, Huang RY. Study of the properties of inorganic elements in atmospheric particulate matter. Environ Sci Technol. 2006;6:49–51.
19. Khramchenkova R, Ionescu C, Sitdikov A, Kaplan P, Gál Á, Gareev B. A pXRF In Situ Study of 16th–17th Century Fresco Paints from Sviyazhsk (Tatarstan Republic, Russian Federation). Minerals. 2019;9:114.
20. Walters VA, de Paula JC, Bard RS, Bard RR, González-Montiel GA, Cornejo Ochoa C, Matheson T, Olson J, Nguyen A, Ile D, Hicks AK, Gushtyuk E, Foronda M, Chávez Álvarez E, Cau Ontiveros MÁ. Portable Raman and XRF analyses of pigments in a 15th-century Mallorcan altarpiece from the Oratorio de Santa Ana in Alcúdia, Spain. J Archaeol Sci Rep. 2022;43:103442.
21. Barone G, Mazzoleni P, Cecchini A, Russo A. In situ Raman and pXRF spectroscopic study on the wall paintings of Etruscan Tarquinia tombs. Dyes Pigm. 2018;150:390–403.
22. Ceccarelli S, Guarneri M, Romani M, Giacopini L, Francucci M, Ciaffi M, De Collibus MF, Puiu A, Verona-Rinati G, Colao F, Fantoni R. Are the blue daemons really blue? Multidisciplinary study for the colours characterization of the mural paintings inside the Blue Daemons Etruscan tomb. J Cult Herit. 2021;47:257–64.
23. Dudgeon K. Insights into resource management and technological development through microbotanical and geoarchaeological characterisation of floor plasters from Neolithic Abu Hureyra, Syria, 8600–6000 cal BC. Quaternary Int. 2023;655:55–68.
24. Isca C, Casoli A, Lopes V, Volpin S. The painting technique of Konrad Witz: an example of experimentation with innovative materials in 15th century. Microchem J. 2023;185: 108236.
25. Li Y, Wang F, Ma J, He K, Zhang M. Study on the pigments of Chinese architectural colored drawings in the Altar of Agriculture (Beijing, China) by portable Raman spectroscopy and ED-XRF spectrometers. Vib Spectrosc. 2021;116: 103291.
26. Sáez-Hernández R, Antela KU, Gallello G, Cervera ML, Mauri-Aucejo AR. A smartphone-based innovative approach to discriminate red pigments in roman frescoes mock-ups. J Cult Herit. 2022;58:156–66.
27. Lv JR. Review of urban atmospheric dust fall research methods. Environ Devel. 2012;24:54–9.
28. Qian GQ, Dong ZB. Research on atmospheric dust collection methods and related issues. J Desert Res. 2004;6:779–82.
29. Lou BY, Ran M, Peng SJ. Chemical issues in heritage conservation research. Chem Educ. 2005;7:1–4.
30. Clark RJH, Hark RR, Salvado N, Butí S, Pradell T. Spectroscopy study of mural paintings from the Pyrenean Church of Saint Eulalia of Unha. J Raman Spectrosc. 2010. https://doi.org/10.1002/jrs.2687.
31. Yang B. Analysis of smoke from burning of major tree species in the Greater Hing'an Mountains and its effect on seed germination. Harbin: Northeast Forestry University; 2020.
32. Bezur A, Lee L, Loubser M, Trentelman K. Handheld XRF in Cultural Heritage. Los Angeles: Getty Conservation Institute; 2020.
33. de Queiroz Baddini AL, de Paula Santos JLV, Tavares RR, de Paula LS, da Araújo Filho HC, Freitas RP. PLS-DA and data fusion of visible Reflectance, XRF and FTIR spectroscopy in the classification of mixed historical pigments. Spectrochimica Acta Part A Mol Biomol Spect. 2022;265:120384.

Publisher's Note